Received: 6 November 2019 | Revised: 18 July 2020 | Accepted: 24 July 2020

DOI: 10.1002/eng2.12266

RESEARCH ARTICLE

WILEY

Deciphering the importance of graded poling in piezoelectric materials: A numerical study

Raj Kiran[1] | **Anuruddh Kumar**[2] | **Saurav Sharma**[1] | **Rajeev Kumar**[1] | **Rahul Vaish**[1]

[1]School of Engineering, Indian Institute of Technology Mandi, Suran, India

[2]School of Electrical Engineering and Biotechnology, Hanyang Institute of Technology, Hanyang University, Seoul, South Korea

Correspondence
Rahul Vaish, School of Engineering, Indian Institute of Technology Mandi, Suran, Himachal Pradesh 175 005, India.
Email: rahul@iitmandi.ac.in

Abstract

Piezoelectric materials play an important role in powering nano and microelectromechanical systems. However, these are often limited by their low sensing, actuation, and power outputs. This study proposes a novel poling direction arrangement theoretically in the piezoelectric materials which enhances the output parameters drastically. The poling angle was graded from bottom to top surface of element in linear fashion which helps in utilizing the bending and shear stresses efficiently. The sensing, actuation and energy harvesting performance of $Pb[Zr_xTi_{1-x}]O_3$ in graded mode was compared with those obtained from operating in transverse and shear modes. It was found from finite element simulations that a maximum sensing voltage of 11.85 V was been obtained in graded mode which was around 15 times higher than that obtained in shear mode. Likewise, a maximum strain of 8.2 μm/m and a tip displacement of 34.3 μm was observed in the graded mode. Eventually, the maximum power of 0.12 W was harvested from graded mode harvester followed by shear mode harvester where only : 1.6×10^{-3} W could be harvested. However, the associated challenge with such study is the fabrication and graded poling of piezoelectric which still is an unexplored research area for scientific fraternity.

KEYWORDS

graded poling, piezoelectricity, shear mode, transverse mode

1 | INTRODUCTION

Since the discovery of piezoelectric materials, researchers, and scientists have carried out extensive research to understand the origin and implication of the piezoelectric effect.[1-4] Research community has shown great interest in these materials due to their inherent ability to convert mechanical strain into electric potential and vice versa.[5-8] Thereby, these materials have seen a huge application in the field of sensors, filters, accelerators, and so on. In particular, till date, the piezoelectric materials have been widely employed for sensing, actuation, and energy harvesting applications.[9-15] Though significant research has been carried out in this field still the performance of piezoelectric materials is often limited by several factors[16-21] and there is always a need to enhance it for sensing, actuation, and energy harvesting applications.

From literature review, it is found that for aforementioned applications, piezoelectric materials are attached to a cantilever beam acting as a host structure.[22-24] In most of the studies, the mode of operation for piezoelectric materials has

been reported to be transverse (d_{31}) mode due to ease of fabrication.[7,25,26] However, in addition to transverse mode other modes such as longitudinal (d_{33}) and shear (d_{15}) have also been explored with a motivation to enhance the output parameters. Caliò et al[27] have conducted a comprehensive study to understand the effect of these three different operating modes. It is evident that poling direction in transverse (d_{31}) and longitudinal (d_{33}) modes are same while the strains are induced in two different directions. On the other side, in shear (d_{15}) mode, poling process is carried out along the length of piezoelectric materials. Due to significant difference in values of piezoelectric coefficients, contrasting difference in output parameters is found during operation.

In spite of extensive research has been carried out to explore the different modes of operation, prime focus of the researchers has been captured by the longitudinal piezoelectric strain coefficient. Surprisingly, numerical values for transverse mode have not been reported for several materials despite of being the most commonly mode employed for sensing, actuation, and energy harvesting applications. As per our literature survey, the maximum values of transverse, longitudinal and shear piezoelectric coupling coefficients have been reported to be −320, 697, and 407 pC/N, respectively, for polycrystalline materials.[28-30] Therefore, it is clear that the value of transverse coefficient is comparably less than other two modes. To this end, optimum piezoelectric properties have been reportedly to be achieved by changing the crystallographic composition, orientation, and through domain engineering.[31]

Several strategies ranging from material and design modification to addition of external circuits have been adopted by the researchers to enhance the performance of the piezoelectric materials. Recently, much attention has been given to the construction of the phase boundaries driven by the composition modifications.[20,32] In one of the researches, Zheng et al[33] claimed that the longitudinal piezoelectric strain coefficient of (K,Na)NbO_3 based ceramics could be enhanced by constructing a new phase boundary (rhombohedral-tetragonal). They established that the higher tetragonal phase fraction can warrant a higher piezoelectric strain coefficient. The strategy of doping the piezoelectric materials with ions has also captured a lot of interest of scientific community. Some studies propound that the piezoelectric performance and temperature stability can be drastically enhanced by chemical doping and interface modifications.[34,35] Another much explored technique to boost the performance is the interfacing of the piezoelectric devices with the power processing circuits. Several researchers have reported that the power from the piezoelectric elements can be enhanced up to 900% using power processing circuits such as synchronized switch harvesting.[36-38] However, the polarization of the piezoelectric material has attracted the attention from researcher in the recent years, as a probable way to tailor and/or enhance the performance of these materials. Yang et al[39] employed the combination of domain engineering and defect engineering by strategically controlling the poling process. The dynamic simulation of domain formation during poling was simulated. The effect of polarization electric field in a porous piezoelectric material on the piezoelectric and dielectric properties was investigated by Martínez-Ayuso et al.[40] Utilizing the electrical and mechanical domain engineering, Wu et al[41] realized d_{36} coefficient in bismuth scandium-lead titanate ceramics, operating in face shear mode. A quantitative domain engineering method was established for precisely designing the domains in a piezoelectric material for enhanced performance.

In the light of the above literature review, it can be concluded that several strategies have been explored so far to enhance the performance of the piezoelectric materials. However, to the best of the authors' knowledge there is no study dealing with the concept of graded poling. Subsequently, it will be demonstrated that at the bottom of the graded poling is the variation of piezoelectric strain coefficients with the poling angle. Recently, some of the researchers have demonstrated the effect of orientation of polarization vector on the sensing, actuation, and energy harvesting of the piezoelectric materials.[42,43] In this direction, this study extends the idea of poling tuning by varying the direction of poling vector throughout the piezoelectric element. This is one of the unique strategies to enhance the piezoelectric performance by utilizing all three modes simultaneously. It is to be noted that the piezoelectric materials attached to host structures operating in transverse mode produce sensing voltage and power only because of bending stresses developed in the structure. These host structures are the evil necessity for operation in transverse mode as they drastically reduce the power density of the piezoelectric harvesters. In addition, these configurations make use only of bending stresses while the shear stresses developed in the structure do not make any significant contribution. On contrary, shear mode-based harvesters rely only on the shear stresses induced which are mainly confined only near the mid-plane region of cantilever configuration subjected to bending. Thus, it gives the motivation to capture all the stresses developed in the material for improvement in the performance of the piezoelectric materials. Therefore, for the first time the concept of graded poling has been introduced theoretically in literature. Using this concept, authors aim to utilize the bending compressive and tensile stresses at the top and bottom of the cantilever-based structures and shear stresses in the mid-section. In addition, no host structure has been taken into the consideration and a comparison has been drawn in between three modes, namely: transverse, shear, and graded modes in terms of sensing, actuation, and harvesting capabilities.

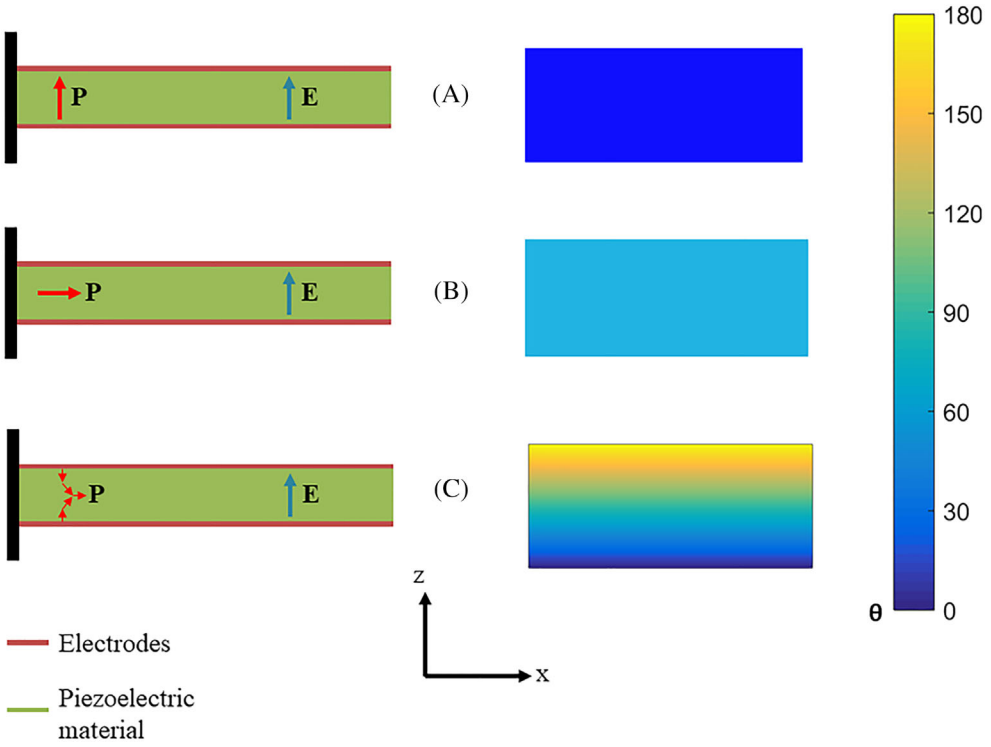

FIGURE 1 Schematic representation of the poling direction in A, transverse, B, shear, and C, graded mode

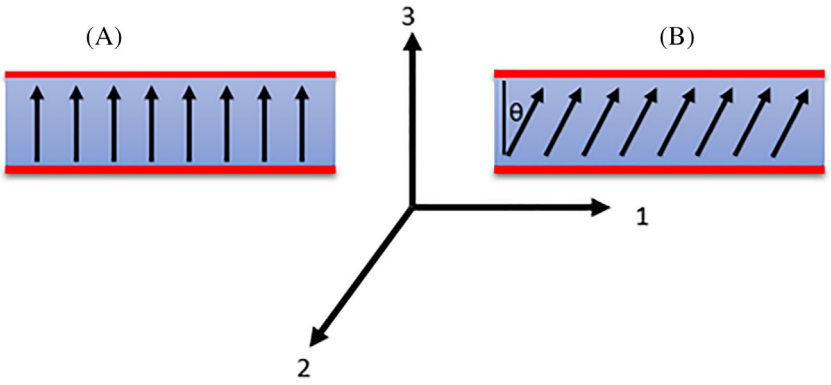

FIGURE 2 Schematic representation of piezoelectric poling, A, along third direction and B, along an arbitrary angle θ

2 | METHODOLOGY

In the present study, we make a comparative study between three different modes in terms of output parameters: sensing voltage, strain, and power harvested. The poling directions have been presented in Figure 1 where Figure 1A-C depict the poling in transverse, shear, and graded mode, respectively. To quantify the effects of graded poling first it becomes imperative to understand the effect of poling orientation on piezoelectric coupling coefficients and dielectric constants. Typically, the piezoelectric materials are poled along third direction as shown in Figure 2A. However, in subsequent sections, it has been assumed that the polarization vector has been rotated by angle θ counter-clockwise about z-axis (third axis) (presented in Figure 2B).

The detailed derivation of the effect of poling angle on the properties has been presented in Appendix I. Upon rotation, it has been found out that the piezoelectric coupling coefficients can be written as:

$$[d]^{\text{eff}} = \begin{bmatrix} d_{11}^{\text{eff}} & d_{12}^{\text{eff}} & d_{13}^{\text{eff}} & 0 & d_{15}^{\text{eff}} & 0 \\ 0 & 0 & 0 & d_{24}^{\text{eff}} & 0 & d_{26}^{\text{eff}} \\ d_{31}^{\text{eff}} & d_{32}^{\text{eff}} & d_{33}^{\text{eff}} & 0 & d_{35}^{\text{eff}} & 0 \end{bmatrix}.$$

TABLE 1 Material properties of PZT (compliance coefficients S_{ij} pm^2/N, piezoelectric coupling coefficients d_{ij} pm/V, relative permittivity at constant stress ε_{ij}^{T}, and density ρ kg/m^3)

S_{11}	S_{12}	S_{13}	S_{33}	S_{44}	S_{66}	d_{31}	d_{15}	d_{33}	ε_{11}^{T}	ε_{33}^{T}	ρ
16.4	−5.7	−7.2	18.8	47.5	44.3	−171	584	374	1730	1700	7750

Out of several coupling coefficients, coefficients relevant to this particular study are given as:

$$d_{31}^{\text{eff}} = \cos(\theta)[d_{31}\cos^2\theta + d_{33}\sin^2\theta - d_{15}\sin^2\theta], \tag{2}$$

$$d_{33}^{\text{eff}} = \cos(\theta)[d_{33}\cos^2\theta + d_{31}\sin^2\theta + d_{15}\sin^2\theta], \tag{3}$$

$$d_{35}^{\text{eff}} = -\sin(\theta)[-d_{33}(1+\cos 2\theta) + d_{31}(1+\cos 2\theta) + d_{15}\cos 2\theta]. \tag{4}$$

These are the effective coupling coefficients at a given particular poling angle. For a piezoelectric material poled along the length (operating in shear mode) piezoelectric coupling coefficient matrix is given as:

$$[d]_{\text{shear}}^{\text{eff}} = \begin{bmatrix} d_{33} & d_{31} & d_{31} & 0 & 0 & 0 \\ 0 & 0 & 0 & 0 & 0 & d_{15} \\ 0 & 0 & 0 & 0 & d_{15} & 0 \end{bmatrix}.$$

However, present study considers the gradation of poling angle from bottom to top surface in a linear fashion as depicted in Figure 1C. Considering the variation of poling angle from 0° to 180°, poling orientation at any height h can be given as:

$$\theta = \frac{\pi}{H}h, \tag{6}$$

where H is the height of the piezoelectric sample.

Therefore, relevant effective piezoelectric coefficients for a linearly graded poled piezoelectric material are given as:

$$d_{31}^{\text{eff}} = \cos\left(\frac{\pi}{H}h\right)\left[d_{31}\cos^2\left(\frac{\pi}{H}h\right) + d_{33}\sin^2\left(\frac{\pi}{H}h\right) - d_{15}\sin^2\left(\frac{\pi}{H}h\right)\right], \tag{7}$$

$$d_{33}^{\text{eff}} = \cos\left(\frac{\pi}{H}h\right)\left[d_{33}\cos^2\left(\frac{\pi}{H}h\right) + d_{31}\sin^2\left(\frac{\pi}{H}h\right) + d_{15}\sin^2\left(\frac{\pi}{H}h\right)\right], \tag{8}$$

$$d_{35}^{\text{eff}} = -\sin\left(\frac{\pi}{H}h\right)\left[-d_{33}\left(1+\cos\left(2\frac{\pi}{H}h\right)\right) + d_{31}\left(1+\cos\left(2\frac{\pi}{H}h\right)\right) + d_{15}\cos\left(2\frac{\pi}{H}h\right)\right]. \tag{9}$$

To emphasize and compare the effect of graded poling, we have considered the most commonly used piezoelectric material $Pb[Zr_xTi_{1-x}]O_3$ (PZT) in this study. The material parameters of PZT are given in Table 1. A piezoelectric element of dimensions 20 cm × 5 cm × 5 mm was taken for the simulation purposes. In addition, to predict the sensing voltage and energy harvested a tip load of 1N was applied while a potential difference of 100 V was applied along the thickness to compute the actuation behavior of the piezoelectric in all three modes.

In present study, finite element method (FEM), one of the most common and effective numerical techniques has been used to simulate the response of piezoelectric element. Plethora of literature is available where FEM has been studied to compute the static and dynamic response of piezoelectric materials.[44-47] Using Hamilton's principle, the coupled equation of motion for piezoelectrics is given as Reference 48:

$$[M_{uu}]\{\ddot{u}\} + [C_{uu}]\{\dot{u}\} + [K_{uu}]\{u\} + [K_{u\varphi}]\{\varphi\} = \{F\}, \tag{10}$$

$$[K_{\varphi u}]\{u\} + [K_{\varphi\varphi}]\{\varphi\} = \{Q\}, \tag{11}$$

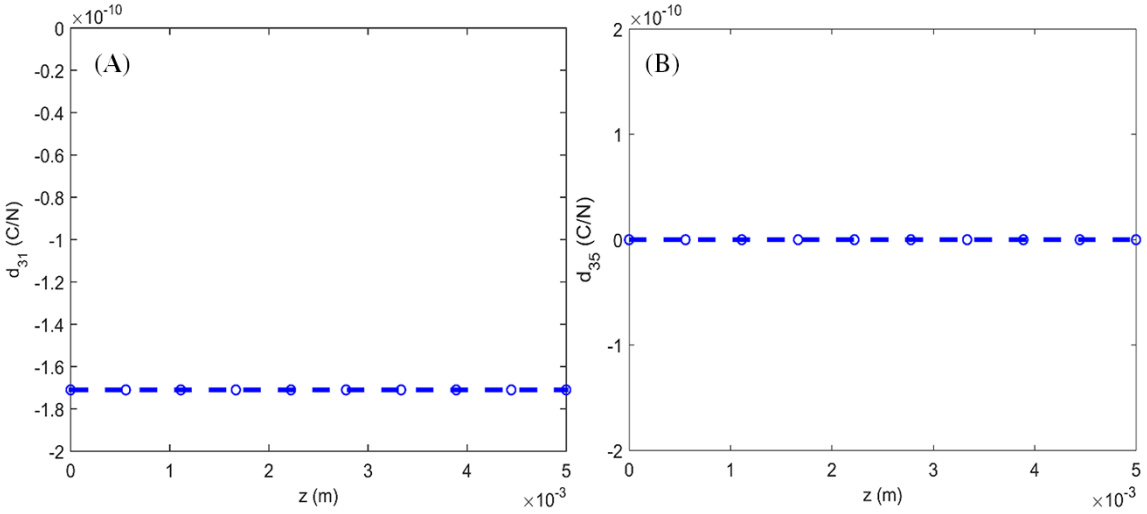

FIGURE 3 Variation of A, transverse (d_{31}^{eff}) and B, shear (d_{35}^{eff}) piezoelectric coupling coefficients along the thickness of piezoelectric element operating in transverse mode

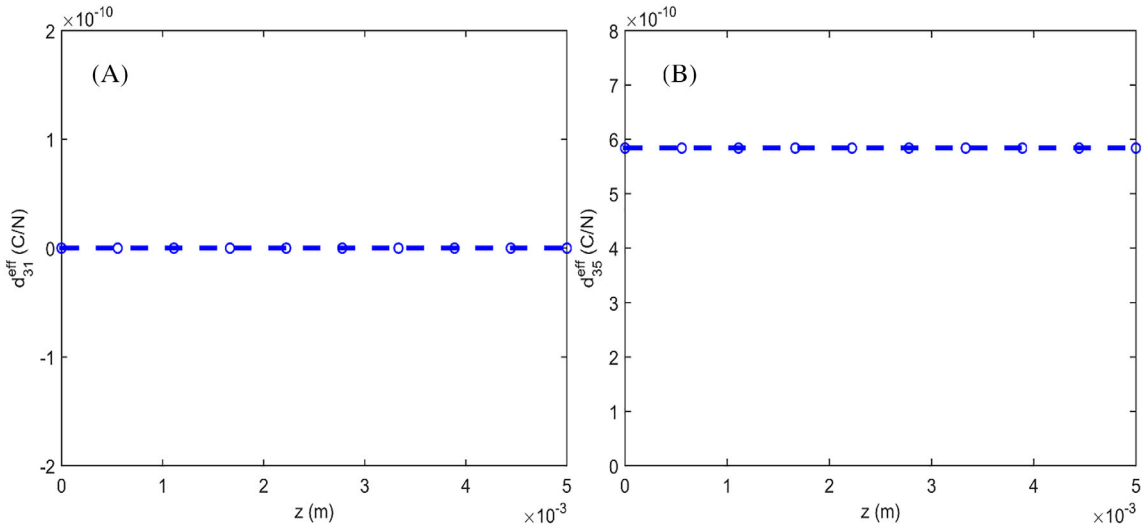

FIGURE 4 Variation of A, transverse (d_{31}^{eff}) and B, shear (d_{35}^{eff}) piezoelectric coupling coefficients along the thickness of piezoelectric element operating in shear mode

where K_{uu} is mechanical stiffness matrix, $K_{u\varphi}$ is the direct piezoelectric coupling matrix, $K_{\varphi\varphi}$ is the dielectric stiffness matrix, $K_{\varphi u}$ the inverse piezoelectric coupling matrix, u the element nodal displacement vector, φ the electric potential vector, F the external force vector, and Q the external electric charge.

Piezoelectric materials act as a sensor when subjected to mechanical stress. It is assumed that no external charge is given to the system which results in the sensing voltage which is given as:

$$\{\varphi\} = -[K_{\varphi\varphi}]^{-1}[K_{\varphi u}]\{u\}. \tag{12}$$

Likewise, during actuation, the displacement field can be computed using the relationship:

$$\{u\} = -[K_{\varphi u}]^{-1}[K_{\varphi\varphi}]\{\varphi\}. \tag{13}$$

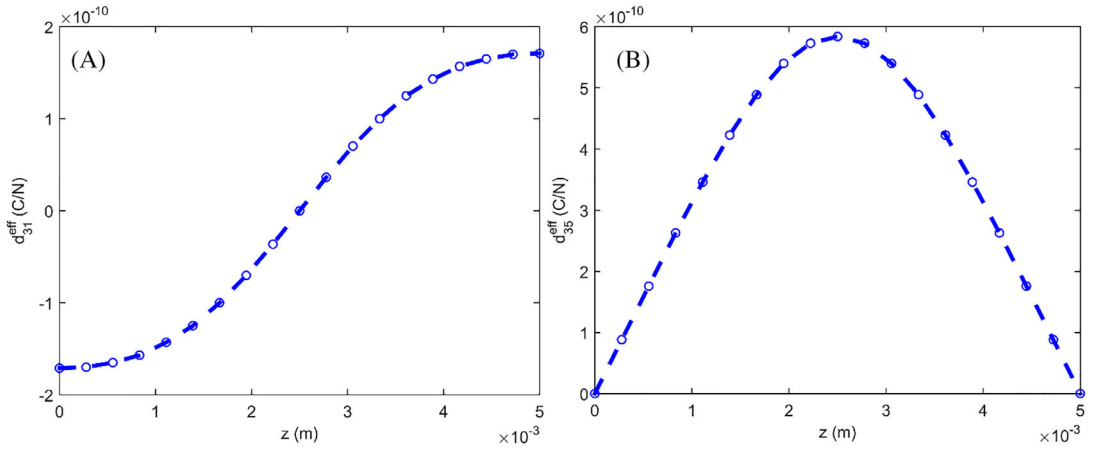

FIGURE 5 Variation of A, transverse (d_{31}^{eff}) and B, shear (d_{35}^{eff}) piezoelectric coupling coefficients along the thickness of piezoelectric element operating in graded mode

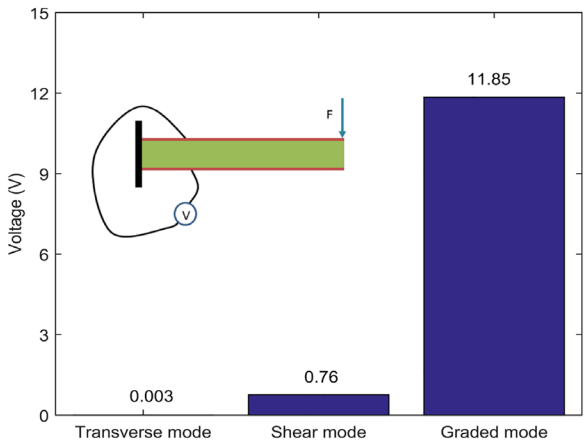

FIGURE 6 Comparison of sensing voltage computed from piezoelectric element operating in transverse, shear, and graded mode

For energy harvesting application, in general, a resistance R is used in the circuit to compute the power. From circuit theory, the current flowing across a resistance is given as:

$$i = \frac{V}{R}. \tag{14}$$

Using Equation (11), we have:

$$\frac{d}{dt}([K_{\varphi u}]\{u\} + [K_{\varphi\varphi}]\{\varphi\}) = \frac{d}{dt}\{Q\}, \tag{15}$$

$$[K_{\varphi u}]\{\dot{u}\}_e + [K_{\varphi\varphi}]_e\{\dot{\varphi}\} + \frac{\{V\}}{R} = 0. \tag{16}$$

Equations (14) and (16) together can be used to compute the current flowing across the resistance and the power generated.

3 | RESULTS AND DISCUSSION

In this section, the graded poling formulation has been implemented in the finite element model and the effect has been realized in three most fundamental applications of piezoelectric materials. In addition, the performance has been compared against the output parameters obtained from the piezoelectric element operating in transverse and shear modes. At

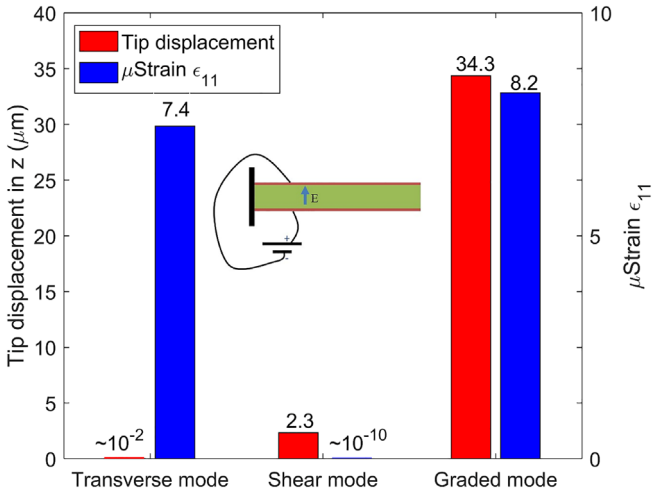

FIGURE 7 Comparison of tip displacement and strain computed from piezoelectric element operating in transverse, shear, and graded mode

the first place, it becomes necessary to identify the variation of the piezoelectric coupling coefficients along the thickness of the sample. The study in later parts will try to corelate the variation of different output parameters with the variation of these coefficients in different modes.

It is evident from Figure 1 that the electrodes are placed in z-direction (or third direction), therefore the major participating modes are d_{31} and d_{35} which produce charge on interaction with bending stress in x-direction and shear stresses in x-z plane. To this end, the variation of d_{31} and d_{35} was plotted as presented in Figure 3A,B, respectively, for the piezoelectric element operating in transverse mode. It is evident that the values are constant across the thickness of the piezoelectric sample since there is no poling grading in the element. It is to be noted that in transverse mode the charge is produced only due to interaction of the bending stress with d_{31} coefficient as all the other piezoelectric coefficients are zero throughout. In nutshell, it can be stated that only the transverse stresses make contribution towards the total polarization.

Likewise, in the element operating in shear mode, d_{31}^{eff} is zero and d_{35}^{eff} is responsible for polarization in shear mode as shown in Figure 4A,B, respectively. The values of the effective piezoelectric strain coefficients are constant through thickness because of the same reason as stated earlier. In this particular case, the electric displacement is observed only due to shear stresses in x-z plane which are dominant in the center region of the beam. Hence, in transverse and shear modes, only one of the stresses either bending or shear stress is utilized for operation while the other is not proper channelized.

Therefore, to fully utilize the stress levels in the structure, it has been poled in graded manner and the variation of d_{31}^{eff} and d_{35}^{eff} has been shown in Figure 5A,B, respectively. It is evident from Equations (7) and (8) that the transverse coupling coefficients get eliminated at the mid-section while the shear coefficient attains it maxima. It is also to be noted that the transverse coefficient gets maximized at the bottom and top surfaces where the shear piezoelectric coefficient is found to be zero. This way shear stresses in the mid-section and the transverse stresses at the top and bottom surfaces of the beam are fully captured. It should also be highlighted at this point that the variation of d_{31}^{eff} and d_{35}^{eff} closely resembles with that of transverse and shear stresses in cantilever bean configuration.

As a next step, we investigate the sensing capabilities of the piezoelectric element in three modes as shown in Figure 6. Therefore, a tip load of 1N has been applied at the end and the voltage has been measured across the element as depicted in inset of the figure. It can be followed from the results that the maximum sensing voltage of 11.85 V is obtained from graded mode element while shear mode element yields only 0.76 V and the output voltage of transverse mode is very insignificant. It happens because of the fact that in the graded mode the bending stress which is maximum at the top and bottom surfaces interacts with the transverse coefficient and the shear stress in the center interacts with the shear strain coefficient yielding the maximum output sensing voltage. On the other hand, in transverse mode, no effective charge is produced due to equal and opposite bending stresses on top and bottom surfaces while shear mode yields higher voltage as compared with that obtained from transverse mode due to its higher value.

Thereafter, the effect of poling on actuation is explored in terms of strain and tip displacement. An electric potential difference of 100 V is applied across the electrodes and the strain in x-direction and tip displacement in z-direction are computed for three modes. It is clear from the preceding sections that the applied electric field is in z-direction therefore the strain in x-direction is governed only by d_{31}^{eff} as per piezoelectric actuation equation. Therefore, from Figure 7, it is clear that the maximum strain of 8.2 μm/m is observed for graded mode followed by transverse mode where a comparative value of 7.4 μm/m is computed.

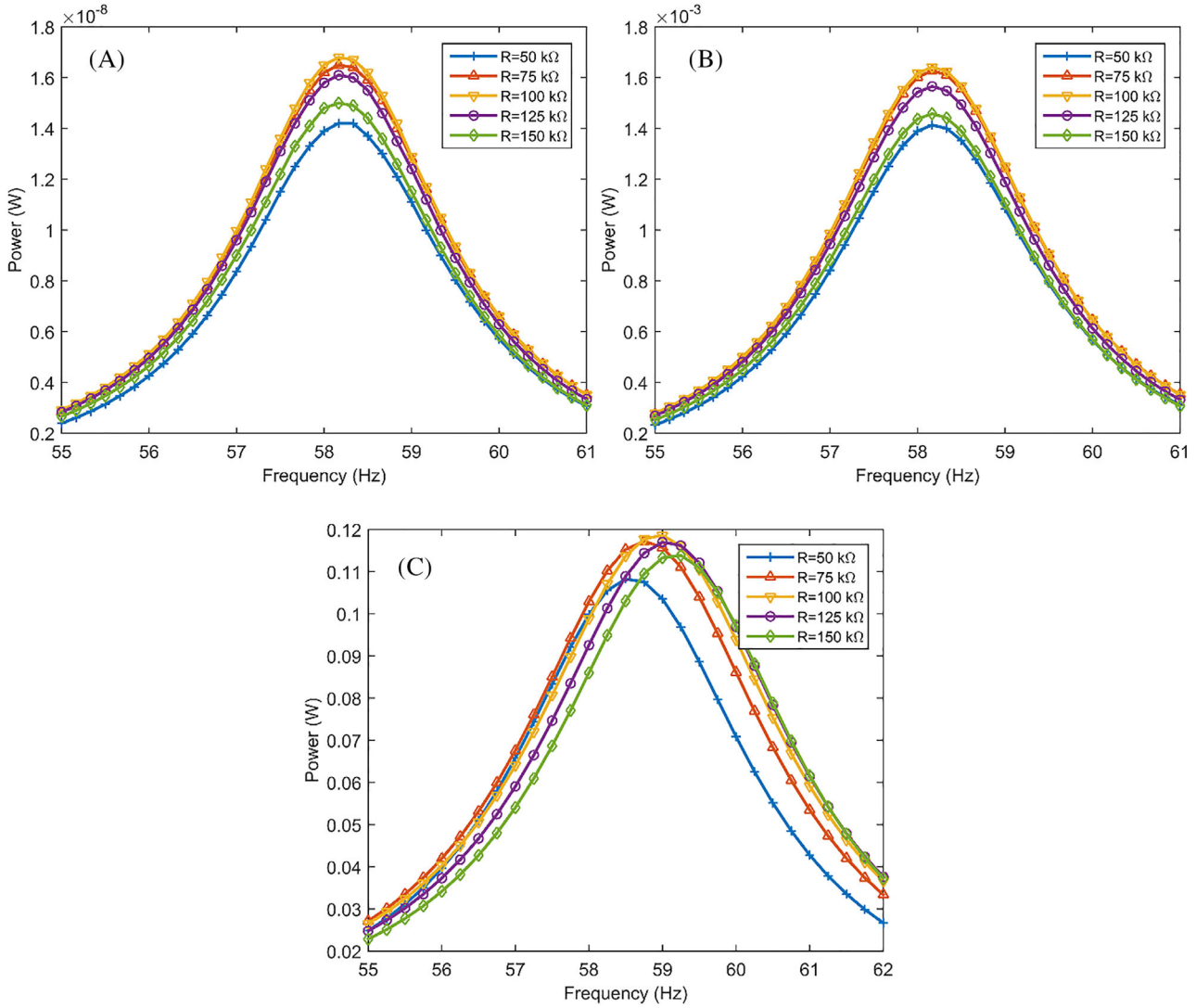

FIGURE 8 Variation of power harvested from piezoelectric element operating in A, transverse, B, shear, and C, graded mode with loading frequency and external resistance

On the contrary, no strain is observed as the effective transverse coefficient gets zero in shear mode. However, interestingly, only a marginal tip displacement in z-direction is observed in transverse mode while tip displacement in shear mode is higher in spite of having negligible strain. This simply implies that the contribution in tip displacement comes not only due to transverse coefficient but also due to shear coefficient. Similar observation is made for graded mode where the tip displacement is a found to be cumulative synergistic effect of transverse and shear coefficients.

Next, the study examines the effect of poling on the energy harvesting. To achieve this end, the beam end has been loaded dynamically at different frequencies and the power generated across different external resistances has been computed as presented in Figure 8. It has been found that the negligible power is produced in transversely poled element as no effective charge is produced upon loading. In case of shear mode, power is produced typically in order of mW which is quite significant as compared with that obtained in the transverse mode. It is also interesting to note that the maximum power is harvested when the mechanical impedance of the system matches well with external applied resistance. Amongst all the modes, the maximum power is achieved in the graded mode for obvious reasons as mentioned earlier and it is at least 100 times higher than that obtained in shear mode.

Eventually, the study also considers the electromechanical factor which is the degree of transduction of mechanical energy into electrical energy or vice versa. Therefore, the displacement has been computed with loading frequency in

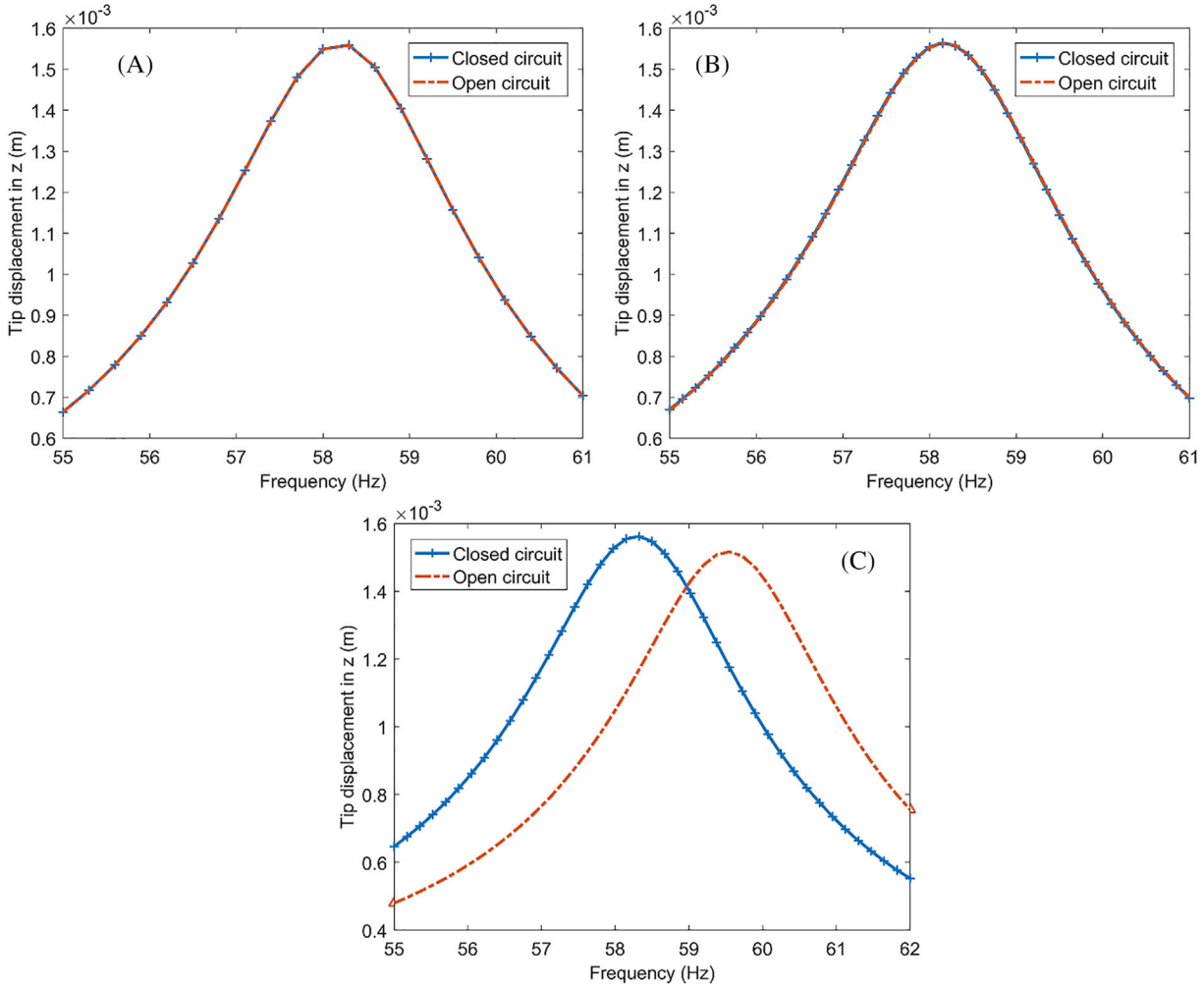

FIGURE 9 Variation of tip displacement in z-direction of piezoelectric element operating in A, transverse, B, shear, and C, graded mode with loading frequency in open and closed-circuit configuration

open and closed-circuit configuration. Electromechanical factor (k) for the piezoelectric materials can be computed from:

$$k^2 = \frac{\omega_{oc}^2 - \omega_{cc}^2}{\omega_{cc}^2}, \tag{17}$$

where ω_{oc} and ω_{cc} are the open circuit and closed-circuit natural frequencies, respectively.

It can be observed from Figure 9 that the electromechanical factor for transverse and shear modes are negligible as there is no significant frequency shift in these two configurations which is in accordance with our previous findings. On the contrary, a significant frequency shift is observed in graded mode piezoelectric element which results in an electromechanical coupling (k) factor of 0.2. It is to be highlighted that this shift is observed due to the electrical stiffening of the piezoelectric material which results in higher natural frequency.

4 | FEASIBILITY ASPECTS

The present concept holds the potential to dramatically improve the overall performance of piezoelectric energy harvesters. However, being a fresh concept, it becomes essential to consider its feasibility in practical application. In this section, we suggest a strategy to achieve the proposed spatial variation of poling direction. When a piezoelectric material sample is electrically poled prior to use, it is subjected to an electric field in the desired direction of poling for a prolonged

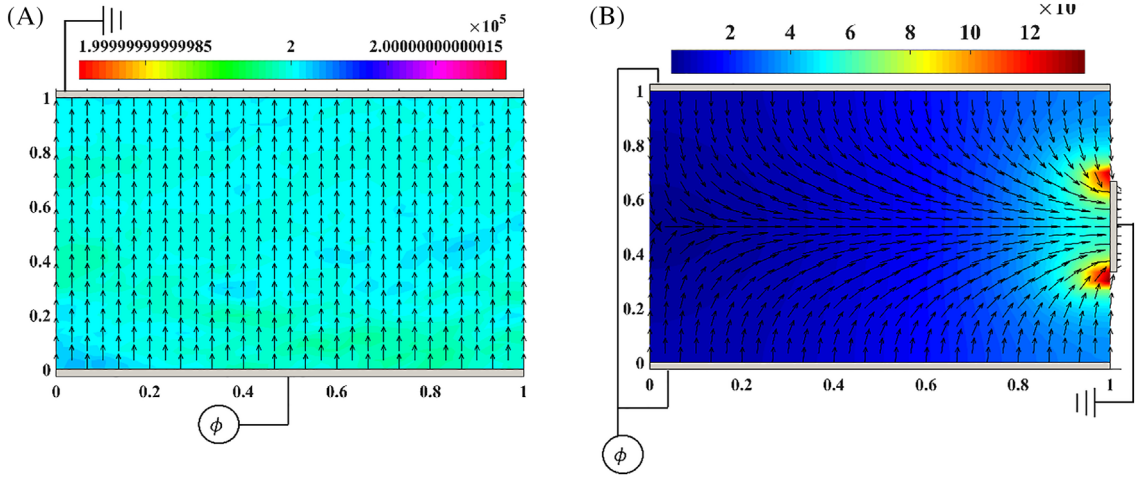

FIGURE 10 Electric field direction (vector map) and magnitude (color map) for A, conventional poling and B, proposed strategy to achieve graded poling

duration. Conventionally this is achieved by placing electrodes on the two opposite faces of the sample, one of which is subjected to an electric potential and the other attached to ground, as shown in Figure 10A. We suggest an alternative approach of electrode placement wherein the right face of the sample is partially connected to ground and top and top faces are applied with an electric potential. The Poisson's equation for 2D electrostatics of the PZT sample is solved by using finite element analysis. Figure 10B schematically shows the electrode placement along with electric field direction at finite element nodes (vector map) and electric field magnitude (color map). The length of the ground electrode in Figure 10B is kept one third of the height of the sample and an electric potential of 2×10^5 V is applied at top and bottom electrodes. The electric field direction at a particular node denotes the orientation of a dipole after poling process. The simulation results shown in Figure 10 are for demonstrating the proposed concept and actual dimensions of the sample and electrode length may influence the poling of the material. The main challenge in applying this technique is of achieving sufficient magnitude of electric field to pole the entire volume (coercive field) and at the same time ensuring that electric field does not cross the breakdown limit of the material. However, existing reports on poling of the piezoelectric material suggest the methods to achieve poling at magnitudes below coercive field value.[49,50] On the other hand, manufacturing techniques have been reported to achieve large electric breakdown strength of ceramics.[51,52] Moreover, the poling direction has also been reported to influence the mechanical properties (fracture toughness and wave propagation characteristics of shells) of piezoelectric materials.[53-57] Poling direction has a varying effect on the wave propagation characteristics of the shells for different stacking sequence, fiber orientation, and axial wave numbers. However, the accurate prediction of effect of proposed poling on mechanical properties of the material requires a separate detailed investigation. The suggested method can provide graded poling similar to that proposed in the present study and validation of the same is likely to be reported in the near future.

5 | CONCLUSIONS

The present study puts forward the concept of graded poling with an objective to utilize the different stresses in the cantilever beam. The poling angle has been graded in a linear manner from the bottom to top surface and has been implemented within the framework of finite element simulations. The new poling scheme has been compared with transverse and shear poling and upon investigation it was found that graded poled piezoelectric element surpassed its counterparts by huge margins in terms of sensing, actuation, and energy harvesting. Thus, the present study paves the path to look into the possibilities of realizing this poling configuration in form of devices such as sensors, vibration-based energy harvesters, and vibration controllers. It is to be highlighted that in spite of having advantages over other modes of operation, the experimental implementation of graded poling is challenging at present. A probable solution for this is proposed by manipulating the electrical boundary conditions during the process of poling. The study provides insight into the novel

proposed concept of graded poling and motivation to the researchers to shift focus towards it so that it can be implemented in real world applications.

PEER REVIEW INFORMATION

Engineering Reports thanks Nan Wu and other anonymous reviewer(s) for their contribution to the peer review of this work.

CONFLICT OF INTEREST

The authors declare that there is no conflict of interest regarding the publication of this article.

AUTHOR CONTRIBUTIONS

Raj Kiran: contributed to the conceptualization; investigation, initail draft writing. **Anuruddh Kumar:** contributed to the conceptualization; investigation; software. **Saurav Sharma:** contributed to the formal analysis; software; writing-review and editing. **Rajeev Kumar:** contributed to the resources. **Rahul Vaish:** contributed to the conceptualization; resources; writing-review and editing.

ORCID

Saurav Sharma https://orcid.org/0000-0002-6158-3057
Rahul Vaish https://orcid.org/0000-0001-7510-7302

REFERENCES

1. Martin RM. Piezoelectricity. *Phys Rev B*. 1972;5:1607-1613. https://doi.org/10.1103/PhysRevB.5.1607.
2. Mason WP. Piezoelectricity, its history and applications. *J Acoust Soc Am*. 1981;70:1561-1566. https://doi.org/10.1121/1.387221.
3. Tagantsev AK. Piezoelectricity and flexoelectricity in crystalline dielectrics. *Phys Rev B*. 1986;34:5883-5889. https://doi.org/10.1103/PhysRevB.34.5883.
4. Furukawa T. Piezoelectricity and pyroelectricity in polymers. *IEEE Trans Electr Insul*. 1989;24:375-394. https://doi.org/10.1109/14.30878.
5. Arnau A, Soares D. Fundamentals of piezoelectricity. *Piezoelectric Transducers Applications*. 2nd. Berlin, Heidelberg: Springer; 2008:1-38. https://doi.org/10.1007/978-3-540-77508-9_1.
6. Schuster A. An introduction to the theory of electricity. *Nature*. 1877;15:526-527. https://doi.org/10.1038/015526a0.
7. Anton SR, Sodano HA. A review of power harvesting using piezoelectric materials (2003-2006). *Smart Mater Struct*. 2007;16:R1-R21. https://doi.org/10.1088/0964-1726/16/3/R01.
8. Uchino K. Piezoelectric ultrasonic motors: overview. *Smart Mater Struct*. 1998;7:273-285. https://doi.org/10.1088/0964-1726/7/3/002.
9. Roundy S, Wright PK. A piezoelectric vibration based generator for wireless electronics. *Smart Mater Struct*. 2004;13:1131-1142. https://doi.org/10.1088/0964-1726/13/5/018.
10. Adhikari S, Friswell MI, Inman DJ. Piezoelectric energy harvesting from broadband random vibrations. *Smart Mater Struct*. 2009;18:115005. https://doi.org/10.1088/0964-1726/18/11/115005.
11. Khan A, Abas Z, Kim HS, Oh IK. Piezoelectric thin films: an integrated review of transducers and energy harvesting. *Smart Mater Struct*. 2016;25:053002. https://doi.org/10.1088/0964-1726/25/5/053002.
12. Park SE, Shrout TR. Ultrahigh strain and piezoelectric behavior in relaxor based ferroelectric single crystals. *J Appl Phys*. 1997;82:1804-1811. https://doi.org/10.1063/1.365983.
13. Zhang S, Li F. High performance ferroelectric relaxor-$PbTiO_3$ single crystals: status and perspective. *J Appl Phys*. 2012;111:111. https://doi.org/10.1063/1.3679521.
14. Sun C, Shi J, Wang X. Fundamental study of mechanical energy harvesting using piezoelectric nanostructures. *J Appl Phys*. 2010;108:034309. https://doi.org/10.1063/1.3462468.
15. Roundy S. On the effectiveness of vibration-based energy harvesting. *J Intell Mater Syst Struct*. 2005;16:809-823. https://doi.org/10.1177/1045389X05054042.
16. Dubus B, Debus JC, Decarpigny JN, Boucher D. Analysis of mechanical limitations of high power piezoelectric transducers using finite element modelling. *Ultrasonics*. 1991;29:201-207. https://doi.org/10.1016/0041-624X(91)90057-F.
17. Dargaville TR, Celina M, Chaplya PM. Evaluation of piezoelectric poly(vinylidene fluoride) polymers for use in space environments. I. Temperature limitations. *J Polym Sci B*. 2005;43:1310-1320. https://doi.org/10.1002/polb.20436.
18. Dargaville TR, Celina M, Martin JW, Banks BA. Evaluation of piezoelectric PVDF polymers for use in space environments. II. Effects of atomic oxygen and vacuum UV exposure. *J Polym Sci B*. 2005;43:2503-2513. https://doi.org/10.1002/polb.20549.
19. Damjanovic D. Materials for high temperature piezoelectric transducers. *Curr Opin Solid State Mater Sci*. 1998;3:469-473. https://doi.org/10.1016/S1359-0286(98)80009-0.
20. Shrout TR, Zhang SJ. Lead-free piezoelectric ceramics: alternatives for PZT? *J Electroceram*. 2007;19:111-124. https://doi.org/10.1007/s10832-007-9047-0.

21. Liu G, Zhang S, Jiang W, Cao W. Losses in ferroelectric materials. *Mater Sci Eng R*. 2015;89:1-48. https://doi.org/10.1016/j.mser.2015.01.002.
22. Fernandes A, Pouget J. Analytical and numerical approaches to piezoelectric bimorph. *Int J Solids Struct*. 2003;40:4331-4352. https://doi.org/10.1016/S0020-7683(03)00222-1.
23. Hwang W-S, Park HC. Finite element modeling of piezoelectric sensors and actuators. *AIAA J*. 1993;31:930-937. https://doi.org/10.2514/3.11707.
24. Wang SY. A finite element model for the static and dynamic analysis of a piezoelectric bimorph. *Int J Solids Struct*. 2004;41:4075-4096. https://doi.org/10.1016/j.ijsolstr.2004.02.058.
25. Beeby SP, Tudor MJ, White NM. Energy harvesting vibration sources for microsystems applications. *Meas Sci Technol*. 2006;17:R175-R195. https://doi.org/10.1088/0957-0233/17/12/R01.
26. Ogawa T, Numamoto Y. Origin of giant electromechanical coupling factor of k_{31} mode and piezoelectric d_{31} constant in $Pb[(Zn_{1/3}Nb_{2/3})_{0.91}Ti_{0.09}]O_3$ single crystal. *Jpn J Appl Phys*. 2002;41:7108-7112. https://doi.org/10.1143/jjap.41.7108.
27. Caliò R, Rongala UB, Camboni D, et al. Piezoelectric energy harvesting solutions. *Sensors (Switzerland)*. 2014;14:4755-4790. https://doi.org/10.3390/s140304755.
28. Liao Y, Sodano HA. Model of a single mode energy harvester and properties for optimal power generation. *Smart Mater Struct*. 2008;17:065026. https://doi.org/10.1088/0964-1726/17/6/065026.
29. Yao Y, Zhou C, Lv D, et al. Large piezoelectricity and dielectric permittivity in $BaTiO_3$-x$BaSnO_3$ system: the role of phase coexisting. *EPL*. 2012;98:27008. https://doi.org/10.1209/0295-5075/98/27008.
30. Pertsev NA, Zembilgotov AG, Waser R. Aggregate linear properties of ferroelectric ceramics and polycrystalline thin films: calculation by the method of effective piezoelectric medium. *J Appl Phys*. 1998;84:1524-1529. https://doi.org/10.1063/1.368218.
31. Tang Y, Zhang S, Shen Z, et al. Primary and secondary pyroelectric coefficients of rhombohedral and tetragonal single-domain relaxor-$PbTiO_3$ single crystals. *J Appl Phys*. 2013;114:084105. https://doi.org/10.1063/1.4819086.
32. Saito Y, Takao H, Tani T, et al. Lead-free piezoceramics. *Nature*. 2004;432:84-87. https://doi.org/10.1038/nature03028.
33. Zheng T, Wu H, Yuan Y, et al. The structural origin of enhanced piezoelectric performance and stability in lead free ceramics. *Energy Environ Sci*. 2017;10:528-537. https://doi.org/10.1039/c6ee03597c.
34. Liu C, Yu A, Peng M, et al. Improvement in the piezoelectric performance of a ZnO Nanogenerator by a combination of chemical doping and interfacial modification. *J Phys Chem C*. 2016;120:6971-6977. https://doi.org/10.1021/acs.jpcc.6b00069.
35. Wang J, Zhou C, Li Q, et al. Simultaneously enhanced piezoelectric properties and depolarization temperature in calcium doped $BiFeO_3$-$BaTiO_3$ ceramics. *J Alloys Compd*. 2018;748:758-765. https://doi.org/10.1016/j.jallcom.2018.03.174.
36. Lallart M, Wu W-J, Yan L, Hung S-W. Inductorless synchronized switch harvesting using a piezoelectric oscillator. *IEEE Trans Power Electron*. 2019;35:2585-2594.
37. Hong J, Chen F, He M, Wang S, Chen W, Guan M. Study of a low-power-consumption piezoelectric energy harvesting circuit based on synchronized switching technology. *Energies*. 2019;12:3166.
38. Asanuma H, Komatsuzaki T, Iwata Y. Increased piezoelectric coupling force in autoparametric excitation harvester connecting to self-powered series and parallel synchronized switch harvesting on inductor (SSHI) interfaces. Paper presented at: Journal of Physics: Conference Series; 2019;12120; Beach, FL: IOP Publishing.
39. Yang C, Sun E, Yang B, Cao W. Modeling dynamic rotation of defect dipoles and poling time dependence of piezoelectric effect in ferroelectrics. *Appl Phys Lett*. 2019;114:102902.
40. Martínez-Ayuso G, Friswell MI, Haddad Khodaparast H, Roscow JI, Bowen CR. Electric field distribution in porous piezoelectric materials during polarization. *Acta Mater*. 2019;173:332-341. https://doi.org/10.1016/j.actamat.2019.04.021.
41. Wu J, Hu Z, Gao X, et al. Quantitative domain engineering for realizing d_{36} piezoelectric coefficient in tetragonal ceramics. *Acta Mater*. 2020;188:416-423. https://doi.org/10.1016/j.actamat.2020.02.031.
42. Gibert JM. Demonstration of the effect of piezoelectric polarization vector on the performance of a vibration energy harvester. *Act Passiv Smart Struct Integr Syst*. 2014;2014(9057):90570L-1-90570L-14. https://doi.org/10.1117/12.2045067.
43. Kiran R, Kumar A, Kumar R, Vaish R. Poling direction driven large enhancement in piezoelectric performance. *Scr Mater*. 2018;151:76-81.
44. S. Narayanan, V. Balamurugan, Finite element modelling of piezolaminated smart structures for active vibration control with distributed sensors and actuators, 2003. https://doi.org/10.1016/S0022-460X(03)00110-X.
45. Pinto Correia IF, Mota Soares CM, Mota Soares CA, Herskovits J. Active control of axisymmetric shells with piezoelectric layers: a mixed laminated theory with a high order displacement field. *Comput Struct*. 2002;80:2265-2275. https://doi.org/10.1016/S0045-7949(02)00239-0.
46. Wang CY, Vaicaitis R. Active control of vibrations and noise of double wall cylindrical shells. *J Sound Vib*. 1998;216:865-888. https://doi.org/10.1006/jsvi.1998.1740.
47. Tan XG, Vu-Quoc L. Optimal solid shell element for large deformable composite structures with piezoelectric layers and active vibration control. *Int J Numer Methods Eng*. 2005;64:1981-2013. https://doi.org/10.1002/nme.1433.
48. Kumar R, Mishra BK, Jain SC. Static and dynamic analysis of smart cylindrical shell. *Finite Elem Anal Des*. 2008;45:13-24. https://doi.org/10.1016/j.finel.2008.07.005.
49. Guo H, Ma C, Liu X, Tan X. Electrical poling below coercive field for large piezoelectricity. *Appl Phys Lett*. 2013;102:6-10. https://doi.org/10.1063/1.4794866.
50. Granzow T, Kounga AB, Aulbach E, Rödel J. Electromechanical poling of piezoelectrics. *Appl Phys Lett*. 2006;88:252907. https://doi.org/10.1063/1.2216028.

51. Huang YH, Wu YJ, Qiu WJ, Li J, Chen XM. Enhanced energy storage density of $Ba_{0.4}Sr_{0.6}TiO_3$-MgO composite prepared by spark plasma sintering. *J Eur Ceram Soc*. 2015;35:1469-1476. https://doi.org/10.1016/j.jeurceramsoc.2014.11.022.
52. Du H-L, Yang Z-T, Gao F. Lead-free nonlinear dielectric ceramics for energy storage applications: current status and challenges. *J Inorg Mater Beijing*. 2018;33:1046-1058.
53. Rattanachan S, Miyashita Y, Mutoh Y. Effect of polarization on fracture toughness of $BaTiO_3/Al_2O_3$ composites. *J Eur Ceram Soc*. 2004;24:775-783. https://doi.org/10.1016/S0955-2219(03)00319-4.
54. Bisheh H, Wu N, Hui D. Polarization effects on wave propagation characteristics of piezoelectric coupled laminated fiber-reinforced composite cylindrical shells. *Int J Mech Sci*. 2019;161-162:105028. https://doi.org/10.1016/j.ijmecsci.2019.105028.
55. Santos e Lucato SL, Lupascu DC, Rödel J. Effect of poling direction on R-curve behavior in lead zirconate titanate. *J Am Ceram Soc*. 2004;83:424-426. https://doi.org/10.1111/j.1151-2916.2000.tb01210.x.
56. Fang F, Yang W. Poling-enhanced fracture resistance of lead zirconate titanate ferroelectric ceramics. *Mater Lett*. 2000;46:131-135. https://doi.org/10.1016/S0167-577X(00)00155-5.
57. Sih GC. A field model interpretation of crack initiation and growth behavior in ferroelectric ceramics: change of poling direction and boundary condition. *Theor Appl Fract Mech*. 2002;38:1-14.

How to cite this article: Kiran R, Kumar A, Sharma S, Kumar R, Vaish R. Deciphering the importance of graded poling in piezoelectric materials: A numerical study. *Engineering Reports*. 2020;2:e12266. https://doi.org/10.1002/eng2.12266

APPENDIX A

In general, the piezoelectric materials are poled in third direction in presented in the article. However, the article takes into account the effect of poling orientation on the piezoelectric strain coefficients. Therefore, the transformation of polarization vector between the coordinate system is to be investigated initially. Polarization vector (P) and stress tensor (T) are coupled to each other through piezoelectric strain coefficients (d) as:

$$P_l = d_{lmn} T_{mn}. \tag{A1}$$

Furthermore, the transformation of the polarization vector from an old coordinate system to a new coordinate system can be formulated as:

$$P' = aP, \tag{A2}$$

where $P^{'}$ and P represent the polarization vectors in new and old coordinate systems, respectively, and a is direction cosines matrix for rotation about any axis and is computed as below:

$$a = \begin{bmatrix} i_1 & j_1 & k_1 \\ i_2 & j_2 & k_2 \\ i_3 & j_3 & k_3 \end{bmatrix},$$

where
$$\begin{array}{lll} i_1 = \cos(x', x) & \mathrm{j}_1 = \cos(y', x) & \mathrm{k}_1 = \cos(z', x) \\ i_2 = \cos(x', y) & \mathrm{j}_2 = \cos(y', y) & \mathrm{k}_2 = \cos(z', y) \\ i_3 = \cos(x', z) & \mathrm{j}_3 = \cos(y', z) & \mathrm{k}_3 = \cos(z', z) \end{array}$$

Substitution of Equation (A1) in Equation (A2) results in

$$P'_l = a(d_{lmn} T_{mn}). \tag{A4}$$

Thereafter, stress tensor (T_{mn}) is also transformed from old coordinate system to a new coordinate system as below:

$$T'_{mn} = QT_{mn}. \tag{A5}$$

Q matrix can also be evaluated using the direction cosines and is given as:

$$Q = \begin{bmatrix} i_1^2 & j_1^2 & k_1^2 & 2j_1k_1 & 2k_1i_1 & 2i_1j_1 \\ i_2^2 & j_2^2 & k_2^2 & 2j_2k_2 & 2k_2i_2 & 2i_2j_2 \\ i_3^2 & j_3^2 & k_3^2 & 2j_3k_3 & 2k_3i_3 & 2i_3j_3 \\ i_2i_3 & j_2j_3 & k_2k_3 & j_2k_3 + k_2j_3 & i_2k_3 + k_2i_3 & j_2i_3 + i_2j_3 \\ i_3i_1 & j_3j_1 & k_3k_1 & j_1k_3 + k_1j_3 & i_1k_3 + k_1i_3 & j_1i_3 + i_1j_3 \\ i_1i_2 & j_1j_2 & k_1k_2 & j_1k_2 + k_1j_2 & i_1k_2 + k_1i_2 & j_1i_2 + i_1j_2 \end{bmatrix},$$

where indices have their usual meanings as in Equation (A3).

Upon substitution of Equation (A5) in Equation (A4) and further simplification results in:

$$P'_l = d'_{lmn} T'_{mn}. \tag{A7}$$

On further simplification, d^{eff}_{lmn} can be defined as:

$$d'_{lmn} = a d_{lmn} Q. \tag{A8}$$

After rotating the poling vector by an arbitrary angle θ about second direction the piezoelectric strain coefficients are found to be dependent on poling angle and are given as presented in Equations (2) to (4) in the article.